Dynamics of single-molecule force-ramp experiments: The role of fluctuations

Douglas B. Staple,* Felix Hanke,† and Hans Jürgen Kreuzer‡
Department of Physics and Atmospheric Science, Dalhousie University, Halifax, NS, Canada B3H 3J5
(Received 27 September 2007; revised manuscript received 6 December 2007; published 25 February 2008)

In the force-ramp mode of the atomic force microscope, the force with which a macromolecule is stretched is increased linearly in time by properly controlling the motion of the cantilever through a feedback loop. Using a master equation approach for the coupled cantilever-macromolecule system, we mimic such a feedback loop, to study nonequilibrium effects in the measurements of force-extension curves and fluctuations. In particular, it is shown that the fluctuations are the same for force-ramp experiments and for the more commonly used constant velocity experiments. Thus the *exact same* statistics suffice for the explanation of either experiment. Specific results are presented for the stretching of Dextran.

DOI: 10.1103/PhysRevE.77.021801 PACS number(s): 36.20.Ey, 82.37.Gk, 82.37.Rs, 82.20.Db

I. INTRODUCTION

The atomic force microscope (AFM) is an ideal tool in polymer science to study the thermodynamics and kinetics of single polymer molecules [1–5]. Quantities of interest and accessible by AFM are the force-extension curve, fluctuations, relaxation times, and nonequilibrium dynamics. Although simple in concept, AFM experiments must be designed judiciously to extract the maximum amount of information from macromolecules. Time scales, length scales, and force regimes are the elements that need careful consideration. This becomes obvious from the fact that the molecule is intricately coupled to the AFM cantilever, and that from the deflection of the latter one extracts both the length of the polymer and the applied force. Whereas the cantilever has a fixed force constant or stiffness (within its harmonic regime), the equivalent segment elasticity $K_s = N(\partial f/\partial L)_T$ of a macromolecule varies continuously from (almost) zero under zero force to infinity at maximum extension or bond rupture; here N is the number of monomers, f is the applied force, and L is the end-to-end length. Thus, any analysis of data and any theory concerned with such experiments must treat the latter as a coupled molecule-cantilever system [6].

In the simplest operational mode of an AFM, one controls the position of the cantilever relative to the substrate to which the molecule is attached, and increases it, for instance, with a constant velocity, $D=vt$. In this situation both the length of the molecule and the force on it are measured, and both fluctuate. On the other hand, in the force-ramp mode one uses a feedback loop to ensure that the applied force increases, for instance, linearly with time, $f=\alpha t$. To obtain such a linearly increasing force, one must control the motion of the cantilever appropriately, i.e., nonlinearly in time. It must be realized that such a feedback system only controls the average force. This can be seen from a comparison of the time scales involved; the macroscopic cantilever position can be mechanically updated on the millisecond time scale, whereas fluctuations in the cantilever deflection occur faster, typically on the microsecond time scale [4,7].

These fluctuations have first been measured for fixed forces by Kawakami *et al.* [8], who calculated the effective spring constant and damping parameter of the polymer-cantilever system in solution under different conditions. Walther *et al.* [4] recently measured the force-extension curve and fluctuations of Dextran stretching, comparing constant velocity and force-ramp modes of their AFM. How well this measurement can be performed in a force-ramp setup depends critically on the cantilever stiffness, the bandwidth of the feedback loop, and the desired rate of force increase [4].

As long as the internal relaxation time of the molecule is shorter than the experimental time scale, the molecule-cantilever system remains in thermal equilibrium. In such cases statistical mechanics can be employed in the Helmholtz ensemble for the coupled system with D the control variable. The main insights from such an analysis are as follows [6]:

(i) For a sufficiently long molecule (with more than 100 monomers typically) any AFM measurement (in equilibrium) will yield the mechanical equation of state of thermodynamics, i.e., the force-extension curve.

(ii) Fluctuations are always given (in the harmonic regime of the cantilever with force constant k_c) by

$$(\delta L)^2 = k_B T/[k_c + (\partial f/\partial L)_T], \quad (\delta f)^2 = k_c^2 (\delta L)^2. \qquad (1)$$

This point is especially important when it comes to comparing force-ramp AFM experiments with those of the constant velocity variety. It will be shown here by various means that the thermal fluctuations are quantitatively the *same in both experiments*.

(iii) For infinitely soft or stiff cantilevers, with $k_c \to 0$ or ∞, the Helmholtz ensemble for the coupled cantilever-molecule system simplifies to the Gibbs or Helmholtz ensemble, respectively, for the isolated molecule.

Infinitely soft or stiff means that the cantilever force constant must be much smaller or much larger than the stiffness of the molecule in the relevant force regime. For the Dextran

*dstaple@dal.ca
†Present address: Fritz-Haber Institut der Max-Planck Gesellschaft, Faradayweg 4-6, 14195 Berlin, Germany. hanke@fhi-berlin.mpg.de
‡Author to whom correspondence should be addressed. h.j.kreuzer@dal.ca

molecules used in Ref. [4] we have in the force range $50\ \text{pN} < f < 1600\ \text{pN}$ a molecule stiffness $10\ \text{pN/nm} < (\partial f/\partial L)_T < 1000\ \text{pN/nm}$. Thus for the cantilevers with $k_c \approx 50\ \text{pN/nm}$ neither limit is reached, and the formulas of Eq. (1) for the coupled system must be used in an analysis of fluctuations.

The usual approach to interpret single-molecule experiments is to use fitting formulas gleaned from very simple analytic models such as the wormlike chain model, the freely jointed chain (FJC) model or *ad hoc* two-state FJC models [5,9]. Such models are usually not thermodynamically consistent, and cannot account for the proper temperature dependence of the system being analyzed [10].

Here we present a complete analysis of the problem, starting from the nonequilibrium statistical mechanics of the coupled molecule-cantilever system [11], employing the continuous two-state model for conformational transitions in Dextran [10]. Specific attention will be given to the question of optimizing the experiment with regard to cantilever stiffness and motion. We will see that, for commonly used cantilevers with stiffness in the range of 100 pN/nm, and force-loading rates of less than 100 nN/s, the molecule is maintained in equilibrium by fast internal relaxation processes. Nonequilibrium effects are predicted for stiff cantilevers and higher pulling speeds.

II. THEORY OF THE COUPLED CANTILEVER-MOLECULE SYSTEM

A. Equilibrium

The statistical mechanics for the coupled cantilever-molecule system has previously been solved for systems with internal relaxation processes which are sufficiently fast to maintain equilibrium throughout the experiment [6]. In this case the distance D of the cantilever from the substrate where one end of the macromolecule is attached is the mechanically controlled variable, and the statistical mechanics of the coupled cantilever-macromolecule system can be treated in the Helmholtz ensemble with the partition function

$$Z_{c\text{-}m}(T,D) = \lambda_m^{-1} \int_0^\infty dL Z_m(T,L) Z_c(T,D-L). \tag{2}$$

Here the subscripts m and c refer to the molecule and the cantilever, respectively, $\lambda_m = h/\sqrt{2\pi\mu k_B T}$ is the thermal wavelength, μ is the mass of a single monomer, and L is the z component of the molecular end-to-end vector, with the z direction perpendicular to the substrate surface.

From Eq. (2) we obtain the Helmholtz free energy of the total system

$$F(T,D) = -k_B T \ln Z_{c\text{-}m}(T,D), \tag{3}$$

which yields the average force on the system

$$\bar{f}(T,D) = -\left.\frac{\partial F(T,D)}{\partial D}\right|_T. \tag{4}$$

As the coupled cantilever-macromolecule system is in internal equilibrium, this is also the force with which the cantilever acts on the macromolecule and vice versa. We obtain for the average length of the macromolecule

$$\bar{L}(T,D) = \frac{\int_0^\infty dL L Z_m(T,L) Z_c(T,D-L)}{\int_0^\infty dL Z_m(T,L) Z_c(T,D-L)}, \tag{5}$$

and for the deflection of the cantilever

$$\bar{L}_c = D - \bar{L}. \tag{6}$$

The force-extension curve of the macromolecule, i.e., $\bar{L}(T,\bar{f})$, is obtained by solving Eqs. (4) and (5) simultaneously for a given temperature and varying the cantilever position D.

To make closer contact with the AFM experiment, we specify the cantilever to be well approximated by a harmonic spring with spring constant k_c. Its canonical partition function is

$$Z_c(T,L_c) = \exp\left(-\frac{1}{2}\beta k_c L_c^2\right). \tag{7}$$

Using the partition function (2) and the length (5), we obtain the average force

$$\begin{aligned}\bar{f}(T,D) &= -\frac{k_B T}{\lambda_m}\frac{1}{Z_{c\text{-}m}}\int_0^\infty dL Z_m(T,L)\frac{\partial}{\partial D}\exp\left(-\frac{\beta k_c}{2}(D-L)^2\right)\\ &= \frac{k_c}{\lambda_m}\frac{1}{Z_{c\text{-}m}}\int_0^\infty dL (D-L) Z_m(T,L) Z_c(T,D-L)\\ &= k_c(D-\bar{L}).\end{aligned} \tag{8}$$

Thus the average force is determined by measuring the average deflection $\bar{L}_c$ of the cantilever as required by (8). Note, in particular, that (5) demonstrates that both the length of the macromolecule and the force needed to maintain this length are fluctuating quantities. For these we have generally

$$(\delta L)^2 = L^2 - \bar{L}^2 = \frac{\int_0^\infty dL (L^2 - \bar{L}^2) Z_m(T,L) Z_c(T,D-L)}{\int_0^\infty dL Z_m(T,L) Z_c(T,D-L)}, \tag{9}$$

and for the harmonic cantilever

$$(\delta f)^2 = k_c^2 (\delta L)^2, \tag{10}$$

so that

$$\frac{\delta f}{\bar{f}} = \frac{\delta L/\bar{L}}{D/\bar{L} - 1}. \tag{11}$$

It has also been shown [6] that the partition function of a stiff cantilever approaches a δ function, and the system partition function goes over into that of an isolated molecule (decoupled from the cantilever) in the Helmholtz ensemble, i.e.,

with fixed length $L=D$ and vanishing length fluctuations. On the other hand, for a very soft cantilever we have $D \gg L$; the force fluctuations become arbitrarily small, so that the system partition function goes over into that of the Gibbs ensemble for an isolated molecule.

B. Kinetics

The standard approach to polymer dynamics in solvent is the Zimm model [12,13], which treats the polymer itself as a set of coupled harmonic oscillators subject to viscous effects due to the solvent, and uses a Langevin equation. The latter is an approximate treatment obtained from a master equation for a Markov process. As we have recently formulated the more general approach via a master equation, which also includes the coupling to the cantilever, we employ this method here as well [11]. This will allow us to account for the conformational transition of Dextran more fully, via the continuous two-state model [10], rather than as a chain of coupled harmonic oscillators. In particular, the effects of activation barriers to conformational transitions are explicitly accounted for.

To study kinetic effects when stretching a macromolecule with an AFM, we use a master equation approach, treating the end-to-end length of the molecule as the stochastic variable [11]. We introduce the probability distribution $P(T,L,D;t)$ that at time t the molecule is stretched to a length L, given that the cantilever is a distance D from the substrate. Its equilibrium value is given by

$$P_{\mathrm{eq}}(T,L,D) = \frac{1}{Z_{c\text{-}m}} Z_m(T,L) \exp\left(-\frac{\beta k_c}{2} (D-L)^2 \right). \quad (12)$$

Treating stretching as a Markov process, the probability satisfies a master equation,

$$\frac{d}{dt} P(T,L,D;t) = \sum_{L'} [W(L,L';D) P(L',D;t) - W(L',L;D) P(L,D;t)], \quad (13)$$

where the transition rates to go from $L \to L'$ are chosen to be symmetric,

$$W(L',L;D) = \sqrt{\frac{Z(L')}{Z(L)}} w_0 \exp\left(-\frac{\beta \Delta (L-L')^2}{b_{0,\mathrm{short}}^2} + \frac{\beta k_c}{4} \times [(D-L)^2 - (D-L')^2] \right), \quad (14)$$

and satisfy detailed balance, hence the appearance of the equilibrium partition functions; here ω_0 is the attempt frequency, Δ is the attempt width, and $b_{0,\mathrm{short}}$ is the equilibrium length of an individual monomer.

In order to obtain a numerical imitation of a cantilever feedback loop, such as is used in a force-ramp AFM, one now must proceed as follows:

(i) At a position D of the cantilever (initially $D=0$) we calculate the partition function $Z_{c\text{-}m}$ for the coupled molecule-cantilever system from (2) and obtain the molecular end-to-end-length, its probability distribution (18), and the average force.

(ii) Using the molecular partition function we calculate the transition rates (14) in the master equation for the updated cantilever position $D+\Delta D$, where ΔD is the distance that the cantilever must move in a time interval Δt, to maintain the constant force-loading rate α.

(iii) The master equation is solved for a time interval Δt starting with initial conditions $P(T,L,D;t)$ to obtain $P(T,L,D+\Delta D;t+\Delta t)$.

(iv) With the latter we calculate the average length and the average force according to Eqs. (5) and (8).

(v) If the force lies above (below) $f=\alpha(t+\Delta t)$ we reduce (increase) D until the prescribed force ramp is achieved. This is our feedback loop.

The result is the following: (a) a linear force ramp $f=\alpha t$ and the time dependence of the cantilever position $D(t)$ required to achieve it; (b) the force-extension curve, fluctuations, etc.

For a wideband feedback loop we must replace step (iv) by the following:

(iv′) From the distribution $P(T,L,D+\Delta D;t+\Delta t)$, randomly select a large number of lengths, calculate the associated force, and average both with this distribution. Then proceed to (v).

A sophisticated experimental feedback loop, as recently implemented with integrating amplifiers [4] will average the input data, as suggested by step (iv) for the cantilever update. This leaves the thermal motion of the cantilever undisturbed by the force-feedback system, and only the average motion of the molecule and cantilever are tracked; this is therefore not a realization of a Gibbs ensemble (constant force) for an isolated molecule. Two different conditions which would in fact give rise to the above ensemble (vanishing force fluctuations) are the limit of a soft cantilever (with respect to the molecule being stretched), and the limit of high bandwidth in the force-feedback system. The first situation has been investigated previously, and is obtainable for some experimental systems [6]. The latter condition, which requires the limit of high feedback bandwidth, implies that the force-feedback loop in such a system could mechanically track and eliminate the fluctuations of a stiff cantilever; this is a daunting challenge considering the mass difference, and is unlikely for cantilevers of experimentally attainable stiffness, considering also the time scales of the optics, electronics, and mechanical linkages involved [4,7].

C. Continuous two-state model for Dextran

Simple models do not account for detailed structure in individual monomer units, and hence cannot predict the conformational transition in Dextran. The Dextran molecule is therefore described with a continuous two-state model [10], where freely jointed monomers are given a length-dependent monomer potential $V(b)$ to account for short (chair) and long (boat) monomers. It has been shown [10] that this approach gives an excellent account of the properties of Dextran. To get the partition function of the molecule in the Helmholtz ensemble (at fixed end-to-end length) we employ the transfer matrix method using the Green function formalism, with the length L as the independent variable. The Green function satisfies the Chapman-Kolmogoroff equation

$$\mathcal{G}_n(L,0) = \int dL' \mathcal{T}(L,L') \mathcal{G}_{n-1}(L',0), \tag{15}$$

where the transfer operator $\mathcal{T}$ specifies the possible lengths or position of a monomer n, given the state of monomer $n-1$. In this particular case, $\mathcal{T}$ is obtained from

$$\mathcal{T}(L,L') = \sum_{i=1}^{N_C} \int_{-1}^{1} d\cos\theta \int_{b_{\min}^{(i)}}^{b_{\max}^{(i)}} db\, \delta(L - L' - b\cos\theta) \times \exp[-\beta V^{(i)}(b)]; \tag{16}$$

for details see Ref. [10]. Notice that the transfer operator (16) is written for general monomer potentials. It is reduced to the continuous two-state model by choosing $N_C=2$ with parabolic $V^{(i)}$. Equations (15) and (16) are then integrated numerically. A molecule consisting of N monomers is described by a Green function $\mathcal{G}_N(L,0)$, which specifies the probability of finding the end of the molecule at a distance L above the substrate.

For the evaluation of observable properties, such as length and force fluctuations, one still must couple the polymer description in the form of $\mathcal{G}_N$ to one of the AFM cantilevers, which in itself is a small statistical system. The conjugated Green function $\mathcal{G}^*(L_c,L)$ for a cantilever with deflection L_c and spring constant k_c is given by

$$\mathcal{G}^*(L_c,L) = \exp\left(-\frac{\beta k_c}{2}(L_c - L)^2\right), \tag{17}$$

from which we can calculate the probability of finding the end of the polymer at some length L as

$$P(L) = \frac{\mathcal{G}^*(L_c,L)\mathcal{G}_N(L,0)}{\int dL' \mathcal{G}^*(L_c,L')\mathcal{G}_N(L',0)}. \tag{18}$$

Any quantity observable with the AFM can be calculated from the moments of the probability density $\langle L^n \rangle = \int dL L^n P(L)$. In particular, the average molecular length $\langle L \rangle$ is the first moment of Eq. (18), which yields the force-extension curve in the Helmholtz ensemble as $\langle f \rangle(\langle L \rangle) = k_c(D - \langle L \rangle)$, for each value of the cantilever deflection L_c.

III. RESULTS

In a previous paper [10], equilibrium results for Dextran, such as the force-extension curve, length fluctuations, and expansion coefficients have already been given, and were shown to agree very well with experimental results. These equilibrium results were obtained from constant velocity experiments performed at such low pulling rates that internal equilibrium was maintained by intramolecular relaxation processes. In this paper, we concentrate on force-ramp experiments on Dextran in and out of equilibrium.

To describe force-ramp experiments with the master equation (13), we must specify the attempt frequency ω_0 and the width Δ in the transition rates (14). They could be obtained by fitting relaxation times, which to our knowledge have not been measured for Dextran. They could also be estimated from activation barriers between the boat and chair configurations. For lack of each we simply take values obtained for DNA relaxation [11], namely, $\omega_0 = 5 \times 10^4\ \mathrm{s}^{-1}$ and $\beta\Delta = \pi$, but we hasten to add that all of our conclusions about nonequilibrium effects for fast force ramps depend on these values; we return to this point in the conclusions.

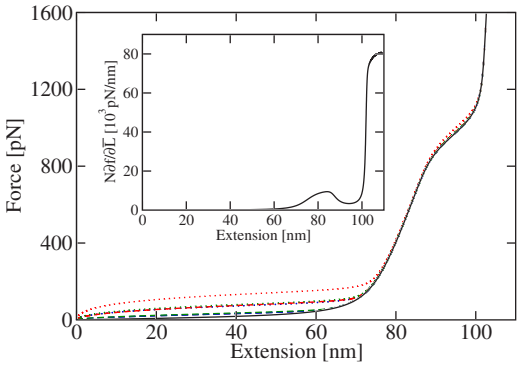

FIG. 1. (Color online) Force-extension curves for Dextran (parameters of the continuous two-state model: $N=175$, $b_{0,\mathrm{short}} = 0.442 \pm 0.12$ nm, $b_{0,\mathrm{long}} = 0.570$ nm [14], $V_{0,\mathrm{long}} - V_{0,\mathrm{short}} = 543 \pm 54$ meV, $k_{\mathrm{short}} = 1.31 \pm 0.22 \times 10^4$ pN/nm, and $k_{\mathrm{long}} = 8.29 \pm 0.04 \times 10^4$ pN/nm [10]). The color scheme and the line types are the same for all figures, namely, black, blue, green, and red lines for cantilever stiffnesses $k_c = 1$, 10, 100, 1000 pN/nm, and solid, dashed, dotted lines for force ramps $\alpha = 1$, 10, 100 nN/s. Of the 12 combinations of α and k_c plotted here, only four distinguishable curves are visible. The top curve is $k_c = 1000$ pN/nm with $\alpha = 100$ nN/s; four curves coincide second from the top, namely, $\alpha = 10$ nN/s, $k_c = 1000$, and the remaining three curves with $\alpha = 100$ nN/s. The bottom (solid and dashed) curves represent the seven remaining combinations of α and k_c, and do not vary by more than 10 pN for a given extension. Inset: segment elasticity of Dextran.

We begin the discussion of examples with soft cantilevers, $k_c < 100$ pN/nm. For force rates $\alpha = 1$, 10, 100 nN/s we "measure" the equilibrium force-extension curve, solid line in Fig. 1. To achieve these force ramps, the cantilever must be moved according to the steepest curves in Fig. 2 (for 1 pN/nm and 10 pN/nm, respectively), which are identical for force rates $\alpha < 100$ nN/s. Recall that the cantilever position is the sum of the molecule extension and the cantilever deflection

$$D(t) = \bar{L} + \bar{L}_c = \bar{L} + \frac{\bar{f}}{k_c}, \tag{19}$$

so that the speed with which it must be moved to get a force ramp with constant slope, $f = \alpha t$, is given by

$$v = \frac{\alpha}{k_c} + \alpha \frac{\partial \bar{L}}{\partial f}, \tag{20}$$

in terms of the inverse of the molecule stiffness $\partial f / \partial \bar{L}$; the latter is shown in the inset of Fig. 1 as the segment elasticity $N \partial f / \partial \bar{L}$ of a system in equilibrium. Note that force and time are equivalent in all figures via $f = \alpha t$; hence to compare the position of the cantilever as a function of time for two dif-

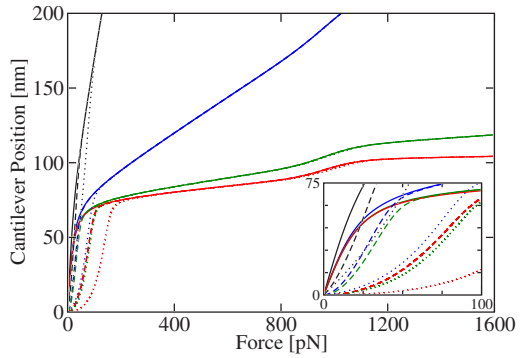

FIG. 2. (Color online) Cantilever motion: Force (or time, via $f=\alpha t$) dependence of cantilever position needed to achieve constant force ramps with various cantilevers, with symbols as in Fig. 1. As in Fig. 1, only five curves differ from the equilibrium results: These are (from right to left) $\alpha=100$ nN/s, $k_c=1000$ pN/nm (dotted red curve), $\alpha=10$ nN/s, $k_c=1000$ pN/nm (dashed red curve), and $\alpha=100$ nN/s, $k_c=100$, 10, and 1 pN/nm (dotted green, blue, and black curves, respectively).

ferent loading rates we must rescale the axes in Fig. 1 for the two different curves via $t=f/\alpha$.

In Fig. 3 we plot $\partial\bar{L}/\partial f=v/\alpha-1/k_c$ as a measure of the velocity (20). As long as the system is maintained in equilibrium, this quantity, plotted as the solid line (black) in Fig. 3, is independent of spring constant k_c and force-loading rate α. At zero force the molecule stiffness is less than these soft cantilevers, but rises quickly, and thus its inverse no longer contributes to the speed for forces larger than about 100 pN, resulting in a perfect force ramp with a constant pulling rate of the cantilever, $\alpha\approx k_c v$.

Picking a cantilever with a stiffness $k_c<100$ pN/nm, the force-extension curves for force rates $\alpha<100$ nN/s are still indistinguishable from the equilibrium curve. For higher

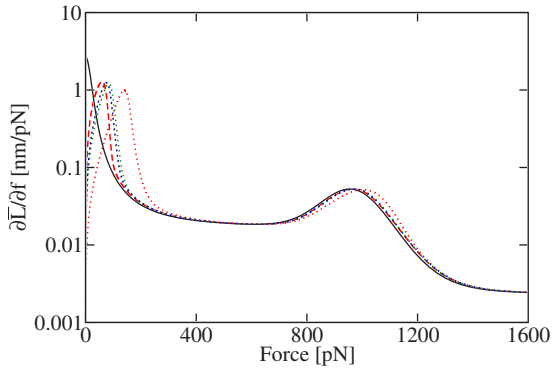

FIG. 3. (Color online) $\partial\bar{L}/\partial f$, obtained by differentiating the curves in Fig. 1. The cantilever speed v needed to produce a constant force ramp $f=\alpha t$ is directly related to this quantity by Eq. (20). The color and symbol coding is the same as in Figs. 1 and 2; the five curves which are distinguishable from the equilibrium (solid curve) result are again (from right to left) $\alpha=100$ nN/s, $k_c=1000$ pN/nm (dotted red curve), $\alpha=100$ nN/s, with $k_c=100$, 10, and 1 pN/nm (dotted green, blue, and black curves, respectively) and $\alpha=10$ nN/s, $k_c=1000$ pN/nm (dashed red curve).

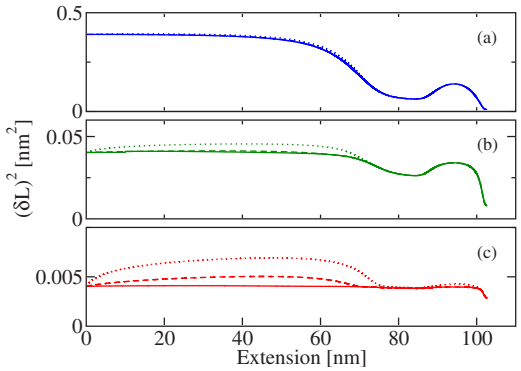

FIG. 4. (Color online) Length fluctuations as a function of extension for various force ramps and cantilever stiffnesses. Because the fluctuations of the softest cantilever ($k_c=1$ pN/nm) are those of equilibrium for all three force rates, we plot in three panels the fluctuations for only the three stiffest cantilevers, $k_c=10$, 100, 1000 pN/nm for panels (a), (b), and (c), respectively. The symbols and colors used are the same as those used in Figs. 1–3, hence the dotted curves represent a loading rate $\alpha=100$ nN/s, the dashed curve represents $\alpha=10$ nN/s, and the solid curves represent a loading rate $\alpha=1$ nN/s.

spring constants, $k_c=100$ pN/nm and $k_c=1000$ pN/nm, the force-extension curve and cantilever motion still only depart from the equilibrium curve for the highest force rates, $\alpha=100$ nN/s, and $\alpha\geq 10$ nN/s, respectively. Hence, for cantilever spring constants and force-loading rates in the range of the present experiment [4], there is no difference in the force-extension relation and corresponding cantilever motion (20) from their equilibrium curves. However, for higher spring constants and force-loading rates, the motion of the cantilever is quite different over the first 100 pN, indicating the presence of nonequilibrium effects (Figs. 2 and 3). The reason why the force-extension curve is not much different is due to the fact that up to 100 pN we are still in the entropic regime, so that small discrepancies can be swamped. The nonequilibrium effects alluded to are most obvious in the cantilever velocity, which no longer starts at a maximum as for the softer cantilever, but takes a finite time to get going.

One of our motivations to look in detail at the dynamics of the force-ramp experiment was the question of how fluctuations in the coupled cantilever-molecule system were affected; these are shown in Fig. 4. First note that the length fluctuations for the slow pulling rates (solid lines) all show a pronounced plateau, which can be attributed to the cantilever limiting the system at small forces, *despite* the force-loading conditions. This situation changes only at large forces, when the polymer itself becomes sufficiently stiff to limit the system beyond the cantilever's effects, in accordance with Eq. (1). This result is in agreement with the measurements of Walther *et al.* on Dextran [4] and also has been measured by Kawakami *et al.* [8]. The latter work contains data on the overall effective spring constant, which also matches the calculations presented here, as well as Eq. (1).

If nonequilibrium effects are encountered, as they are for stiffer cantilevers and higher force rates, they should show up clearly in the fluctuations, as we have shown previously for isolated molecules [11]. Indeed, only for the softest can-

tilever ($k_c=1$ pN/nm) are the fluctuations those of equilibrium for all three force rates. Already for $k_c=10$ pN/nm we see a (minimal) enhancement in the fluctuations for low forces (in the entropic regime) but only at the highest force rate [panel (a) in Fig. 4]. This enhancement becomes dramatic for stiffer cantilevers, panels (b) and (c) in Fig. 4. Note that the major nonequilibrium effect on the fluctuations occurs well below the transition region for Dextran.

IV. DISCUSSION

A master equation approach to the stretching dynamics of a polymer molecule in an AFM allows a detailed analysis and assessment of the various modes of measurement, namely, constant velocity and constant force ramp. In particular, it produces the velocity profile needed for the motion of the cantilever to achieve a constant force ramp. It turns out that for presently used cantilevers, with stiffnesses between 10 and 100 pN/nm, and for force ramps of less than 100 nN/s, internal relaxation processes ensure that the molecule is in internal equilibrium throughout the experiment. Nonequilibrium effects show up for very stiff cantilevers, in the range of 1000 pN/nm, and for high force-loading rates. These effects can be seen in the force-extension curves at low forces (in the entropic regime) as discussed in an earlier paper [11], and also through a considerable increase in the fluctuations, as seen in Fig. 4. However, we conclude that such effects cannot be seen in current experiments.

All of the conclusions reached in this paper regarding the observation of nonequilibrium effects in AFM experiments on macromolecules, and Dextran in particular, are predicated on the choice of the attempt frequency ω_0, which we took from a fit to DNA relaxation times. Because Dextran is much stiffer than DNA (the force needed to induce a conformational transition is higher by an order of magnitude) its attempt frequency should be higher. If that is the case, then nonequilibrium effects should only be observable at yet faster force ramps.

To move into the direction of nonequilibrium experiments it would be highly desirable to measure the molecular relaxation times. This could be done by very fast pulling and then following the relaxation of the molecule as a function of time. A fit with the present theory to the relaxation curve would provide a value for the attempt frequency ω_0 [15].

In a recent paper by Walther *et al.*, results for the stretching of Dextran under constant velocity and force-ramp conditions are presented, including fluctuations. We have shown here that their observations can be fully explained if the fluctuations of the cantilever are included. In general, thermal length and force fluctuations of the AFM cantilever are present in both constant velocity, as well as constant average force-loading rate experiments implemented using force-feedback loops. Hence, if the molecule-cantilever system is maintained in equilibrium throughout both experiments, then one should expect the same results—provided of course that the conditions in the two experiments are otherwise identical. We realize that separately performing these experiments under precisely the same conditions is not possible, but would hope that, by changing only the controlling electronics, constant velocity and constant force-loading rate experiments could be performed successively on a single-molecule-cantilever system, with the expectation of perfect agreement in all experimentally observable quantities.

ACKNOWLEDGMENTS

The calculations presented in this paper were performed on the WestGrid computing resources. This work was supported by grants from NSERC and the Office of Naval Research. One of the authors (D.B.S.) would like to acknowledge support from NSERC. Two of the authors (D.B.S., F.H.) thank the Killam Trusts for support.

[1] M. Rief, F. Oesterhelt, B. Heymann, and H. E. Gaub, Science **275**, 1295 (1997).
[2] M. Rief, M. Gautel, F. Oesterhelt, J. M. Fernandez, and H. E. Gaub, Science **276**, 1109 (1997).
[3] F. Oesterhelt, M. Rief, and H. E. Gaub, New J. Phys. **1**, 6 (1999).
[4] K. A. Walther, J. Brujic, H. Li, and J. M. Fernandez, Biophys. J. **90**, 3806 (2006).
[5] B. S. Khatri, M. Kawakami, K. Byrne, D. A. Smith, and T. C. B. McLeish, Biophys. J. **92**, 1825 (2007).
[6] H. J. Kreuzer, S. H. Payne, and L. Livadaru, Biophys. J. **80**, 2505 (2001).
[7] M. Schlierf, H. Li, and J. M. Fernandez, Proc. Natl. Acad. Sci. U.S.A. **101**, 7299 (2004).
[8] M. Kawakami, K. Byrne, B. Khatri, T. C. B. Mcleish, S. E. Radford, and D. A. Smith, Langmuir **20**, 9299 (2004).
[9] M. Rief, J. M. Fernandez, and H. E. Gaub, Phys. Rev. Lett. **81**, 4764 (1998).
[10] F. Hanke and H. J. Kreuzer, Eur. Phys. J. E **22**, 163 (2007).
[11] F. Hanke and H. J. Kreuzer, Phys. Rev. E **72**, 031805 (2005).
[12] M. Doi and S. F. Edwards, *The Theory of Polymer Dynamics* (Oxford University Press, Oxford, 1986).
[13] A. Y. Grosberg and A. R. Khokhlov, *Statistical Physics of Macromolecules* (AIP, New York, 1994).
[14] P. E. Marszalek, A. F. Oberhauser, Y.-P. Pang, and J. M. Fernandez, Nature (London) **396**, 661 (1998).
[15] F. Hanke and H. J. Kreuzer, Int. J. Quantum Chem. **106**, 2953 (2006).